

## Concurrent Improvement in $J_{SC}$ and $V_{OC}$ in High-Efficiency Ternary Organic Solar Cells Enabled by a Red-Absorbing Small-Molecule Acceptor with High LUMO Level

Tao Liu,<sup>\*a,b</sup> Ruijie Ma,<sup>b</sup> Zhenghui Luo,<sup>\*b</sup> Yuan Guo,<sup>c,d</sup> Guangye Zhang,<sup>e</sup> Yiqun Xiao,<sup>f</sup> Tao Yang,<sup>g</sup> Yuzhong Chen,<sup>b</sup> Gang Li,<sup>a</sup> Yuanping Yi,<sup>c</sup> Xinhui Lu,<sup>f</sup> He Yan<sup>\*b,h</sup> and Bo Tang<sup>\*a</sup>

<sup>a</sup> College of Chemistry Chemical, Engineering and Materials Science, Key Laboratory of Molecular and Nano Probes, Ministry of Education, Collaborative Innovation Center of Functionalized Probes for Chemical Imaging in Universities of Shandong, Institute of Materials and Clean Energy, Shan dong Provincial Key Laboratory of Clean Production of Fine Chemicals, Shandong Normal University, Jinan 250014, P. R. China. E-mail: tangb@sdu.edu.cn

<sup>b</sup> Department of Chemistry and Hong Kong Branch of Chinese National Engineering Research Center for Tissue Restoration & Reconstruction, Hong Kong University of Science and Technology (HKUST), Clear Water Bay, Kowloon, Hong Kong, China. Email: liutaozhx@ust.hk; luozheng@ust.hk; hyan@ust.hk

<sup>c</sup> Beijing National Laboratory for Molecular Science, Key Laboratory of Organic Solids, Institute of Chemistry, Chinese Academy of Sciences, Beijing 100190, P. R. China.

<sup>d</sup> School of Light Industry and Engineering, Qilu University of Technology (Shandong Academy of Science), Jinan 250353, P. R. China.

<sup>e</sup> eFlexPV Limited, Flat/RM B, 12/F, Hang Seng Causeway Bay BLDG, 28 Yee Wo Street, Causeway Bay, Hong Kong.

<sup>f</sup> Department of Physics, Chinese University of Hong Kong, New Territories, Hong Kong, China

<sup>g</sup> Centre for Mechanical Technology and Automation, Department of Mechanical Engineering, University of Aveiro, 3810-193 Aveiro, Portugal.

<sup>h</sup> Hong Kong University of Science and Technology-Shenzhen Research Institute, No. 9 Yuexing first RD, Hi-tech Park, Nanshan, Shenzhen 518057, P. R. China.

## **Solar cell fabrication and characterization**

Solar cells were fabricated in a conventional device configuration of ITO/PEDOT:PSS/active layers/ZrAcac/Al. The ITO substrates were first scrubbed by detergent and then sonicated with deionized water, acetone and isopropanol subsequently, and dried overnight in an oven. The glass substrates were treated by UV-Ozone for 30 min before use. PEDOT:PSS (Heraeus Clevis P VP AI 4083) was spin-cast onto the ITO substrates at 4000 rpm for 30 s, and then dried at 150 °C for 15 min in air. The PM6:acceptors blends (1:1 weight ratio) were dissolved in chloroform (the total concentration of blend solutions were 18 mg mL<sup>-1</sup> for all blends), with the addition of 0.25% DIO as additive, and stirred overnight on a hotplate at 40°C in a nitrogen-filled glove box. The blend solution were spin-cast at 3000 rpm for 40 s on the top of PEDOT:PSS layer followed by a solvent annealing step, which was conducted by placing chloroform in the petri dish for 40s. After solvent annealing, a thermal annealing step at 90 °C for 5 min was performed to remove the residual solvent. A thin Zracac layer was coated on the active layer. was coated on the active layer, followed by the deposition of Al (100 nm) (evaporated under  $5 \times 10^{-5}$  Pa through a shadow mask). The optimal active layer thickness measured by a Bruker Dektak XT stylus profilometer was about 105 nm. The current density-voltage (J-V) curves of all encapsulated devices were measured using a Keithley 2400 Source Meter in air under AM 1.5G (100 mW cm<sup>-2</sup>) using a Newport solar simulator. The light intensity was calibrated using a standard Si diode (with KG5 filter, purchased from PV Measurement to bring spectral mismatch to unity). Optical microscope (Olympus BX51) was used to define the device

area (5.9 mm<sup>2</sup>). IPCEs were measured using an Enlitech QE-S EQE system equipped with a standard Si diode. Monochromatic light was generated from a Newport 300W lamp source.

### **SCLC measurements**

The electron and hole mobility were measured by using the method of space-charge limited current (SCLC) for electron-only devices with the structure of ITO/ZnO/active layer/Zracac/Al and hole-only devices with the structure of ITO/MoO<sub>x</sub>/active layers/MoO<sub>x</sub>/Al. The charge carrier mobility was determined by fitting the dark current to the model of a single carrier SCLC according to the equation:  $J = 9\epsilon_0\epsilon_r\mu V^2/8d^3$ , where  $J$  is the current density,  $d$  is the film thickness of the active layer,  $\mu$  is the charge carrier mobility,  $\epsilon_r$  is the relative dielectric constant of the transport medium, and  $\epsilon_0$  is the permittivity of free space.  $V = V_{app} - V_{bi}$ , where  $V_{app}$  is the applied voltage,  $V_{bi}$  is the offset voltage. The carrier mobility can be calculated from the slope of the  $J^{1/2} \sim V$  curves.

**Atomic force microscopy (AFM).** AFM images were obtained by using a Dimension Icon AFM (Bruker) in a tapping mode.

**GIWAXS characterization.** GIWAXS measurement were carried out with a Xeuss 2.0 SAXS/WAXS laboratory beamline using a Cu X-ray source (8.05 keV, 1.54 Å) and a Pilatus3R 300K detector. The incidence angle is 0.2°. The samples for GIWAXS measurements are fabricated on silicon substrates using the same recipe for the devices.

**GISAXS characterization.** GISAXS was conducted at 19U2 SAXS beamline at Shanghai Synchrotron Radiation Facility, Shanghai, China, using the  $0.15^\circ$  incident angle with 10 keV primary beam.

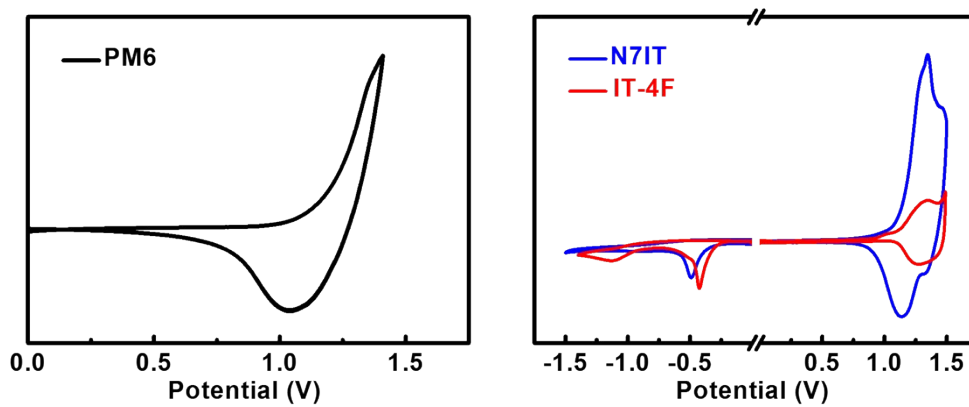


**Figure S1.** The CV curves of PM6, IT-4F and N7IT.

### Appendix: Summary of Certificate

NIM Certificate No.: GXtc2019-0121

DUT S/N: 100-3#-M001

Date of Test: 01/18/2019

Manufacturer: Hong Kong University of Science and Technology

Type: Organic Solar Cells

Temperature Sensor/Control System: None

Mask: An aperture area of 4.638 mm<sup>2</sup> (Certificate No.: CDjc2019-0416)

Environmental conditions at the time of calibration: (20.8±1) °C, RH (22±2) %

The calibration has been conducted by the PV Metrology Lab of NIM (National Institute of Metrology, China). Measurement of irradiance intensity and all other measurements are traceable to the International System of Units (SI). The performance parameters reported in this certificate apply only at the time of the test for the sample.

$I_{sc}$ [mA]	1.054	$V_{oc}$ [V]	0.889	$P_{max}$ [mW]	0.653
$I_{max}$ [mA]	0.895	$V_{max}$ [V]	0.730	Efficiency [%]	14.08
FF [%]	69.71	Area [mm <sup>2</sup> ]	4.638		

#### Methods:

I-V: IEC60904-1: Measurement of photovoltaic current-voltage characteristics  
JJF 1622-2017: Calibration Specification of Solar Cells: Photoelectric Properties

#### Standard Test Conditions (STC):

Spectrum: AM 1.5G (ASTM G173-03/IEC 60904-3 ed.2); 1000 W/m<sup>2</sup> at 25.0 °C.

#### Secondary Reference Cell:

Device S/N: 81#

Device Material: Mono-Si

#### Solar Simulator:

Classification: AAA (Double-light source: Xeon and Halogen)

Total irradiance: 1000 W/m<sup>2</sup> based on  $I_{sc}$  of the above Secondary Reference Cell.

Issue Date	01/18/2019
------------	------------

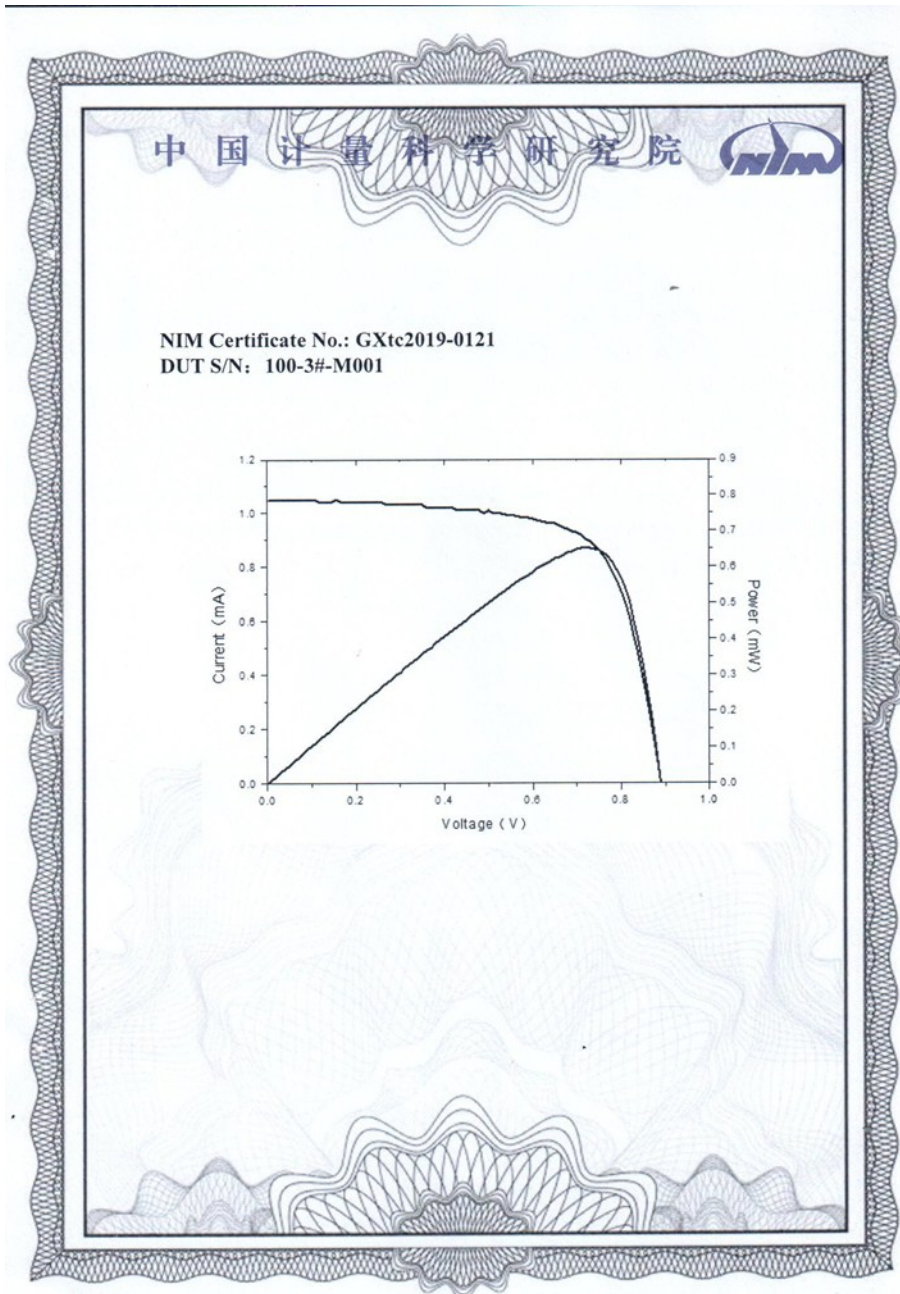


**Figure S2.** Certificate report of a packaged conventional device based on PM6:IT-4F:N71T in National Institute of Metrology, China.

**Table S1.** Photovoltaic parameters of highly efficient ternary organic solar cells based on two nonfullerene acceptors.

Strategy (Characteristics of guest acceptors relative to host acceptors)	Binary host device			Ternary device			Ref
	$V_{oc}$ (V)	$J_{sc}$ ( $\text{mA cm}^{-2}$ )	PCE (%)	$V_{oc}$ (V)	$J_{sc}$ ( $\text{mA cm}^{-2}$ )	PCE (%)	
Similar absorption	0.993	18.47	13.04	0.981	18.42	14.13	1
	0.95	17.90	11.83	0.91	19.60	13.27	2
	0.980	15.29	9.39	0.917	16.89	11.52	3
Blue-shifted absorption and higher LUMO energy level	0.857	25.05	15.45	0.868	25.39	16.51	4
	0.836	17.44	10.51	0.875	17.81	11.92	5
	0.84	25.6	16.0	0.85	26.1	16.7	6
	0.869	22.85	13.70	0.887	22.83	15.06	7
Red-shifted absorption and lower LUMO energy level	0.915	20.27	13.72	0.857	23.99	15.37	8
	0.917	20.17	13.66	0.897	22.35	14.75	9
	0.884	19.94	13.47	0.847	23.66	14.96	10
Red-shifted absorption and higher LUMO energy level	0.90	16.0	9.9	0.87	20.0	12.0	11
	0.869	20.26	13.62	0.890	22.54	15.02	This work
	0.844	25.10	16.49	0.855	25.51	17.07	work

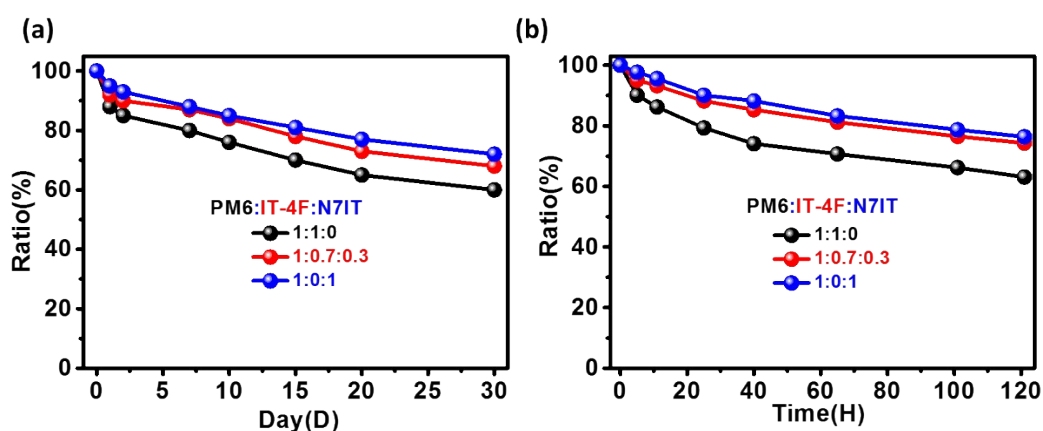


**Figure S3.** Device stability: (a) The PCE reduction of the packaged binary devices and the optimal ternary device during the 30 days stored in air; (b) The photostability of the packaged binary devices and the optimal ternary device during 120 hours devices under LED flood light with a power of 150W.

**Table S2.** The parameters of exciton dissociation efficiency and charge collection

efficiency.

PM6:IT-4F:N7IT	$J_{\text{sat}}$	$J_{\text{ph}}^{\text{a}}$	$J_{\text{ph}}^{\text{b}}$	$\eta_{\text{diss}}$	$\eta_{\text{coll}}$
	(mA cm <sup>-2</sup> )	(mA cm <sup>-2</sup> )	(mA cm <sup>-2</sup> )	(%)	(%)
1:1:0	21.06	20.26	18.62	96.2	88.4
1:0.7:0.3	23.73	22.54	20.02	95.0	84.4
1:0:1	23.51	21.83	18.30	92.9	77.9

a: Under short circuit condition; b: Under the maximal power output condition

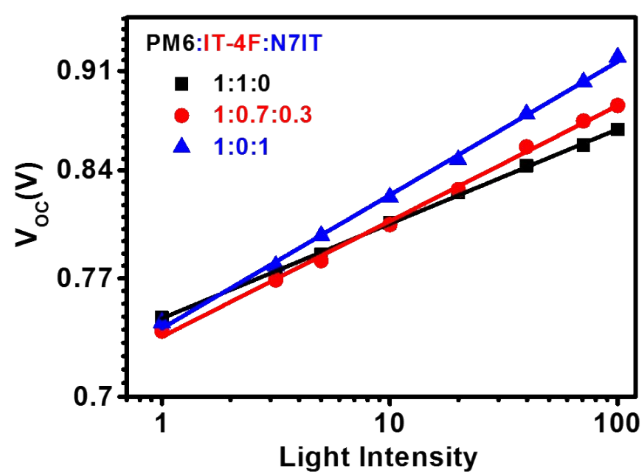


**Figure S4.** Light intensity dependence of  $V_{\text{OC}}$  of the devices based on PM6:IT-4F, PM6:IT-4F:N7IT and PM6:N7IT.

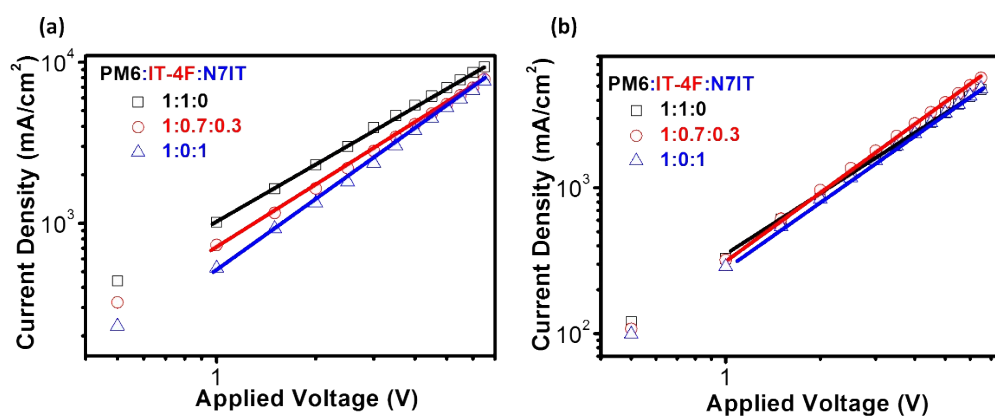


**Figure S5.** (a) PM6:IT-4F:N7IT blend films with different N7IT content in hole-only devices; (b) PM6:IT-4F:N7IT blend films with different N7IT content in electron-only devices.



**Table S3.** The hole and electron mobility of PM6:IT-4F:N7IT blend films with different N7IT content.

N7IT contents	$\mu_h$ ( $\text{cm}^2 \text{V}^{-1} \text{s}^{-1}$ )	$\mu_e$ ( $\text{cm}^2 \text{V}^{-1} \text{s}^{-1}$ )	$\mu_h/\mu_e$
0%	$6.71 \times 10^{-4}$	$4.43 \times 10^{-4}$	1.51
30%	$8.13 \times 10^{-4}$	$4.90 \times 10^{-4}$	1.66
100%	$8.56 \times 10^{-4}$	$4.65 \times 10^{-4}$	1.84

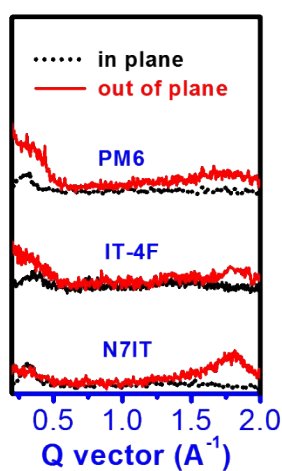


**Figure S6.** GIWAXS intensity profiles of IT-4F, PM6 and N7IT neat films along the in-plane (black lines) and out-of-plane (red lines) directions.

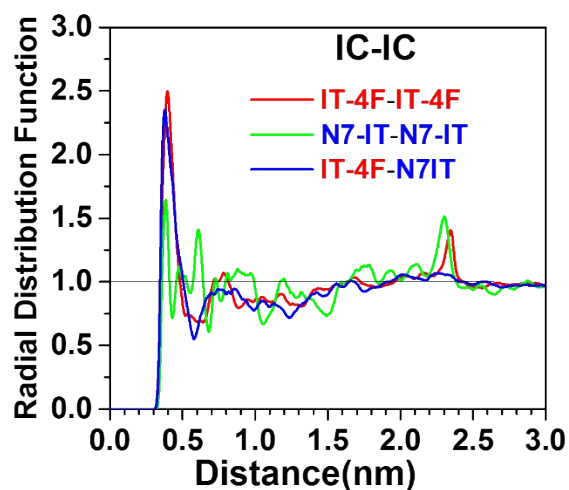


**Figure S7.** Center-of-mass radial distribution functions of the terminal groupS for the IT-4F:IT-4F, N7IT:N7IT and IT-4F:N7IT

**Table S4.** The binding energies ( $\Delta G$ ) at MM and wB97XD/6-31G(d,p) level of theory for all the IT-4F and N7IT pairs extracted from the MD simulations.

	$\Delta G$ (MM)/kcal mol <sup>-1</sup>	$\Delta G$ (DFT)/kcal mol <sup>-1</sup>
IT-4F	-33.08	-28.53
N7IT	-25.68	-20.99
IT-4F:N7IT	-28.65	-25.14

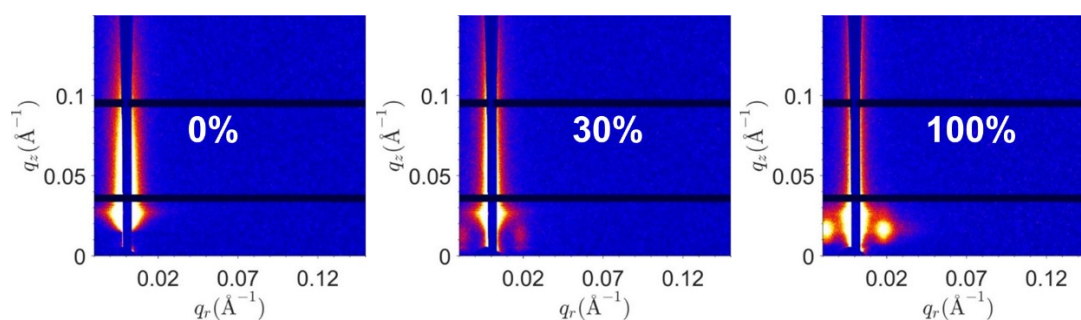


**Figure S8.** 2D GISAXS patterns of the ternary blend films with different N7IT contents.

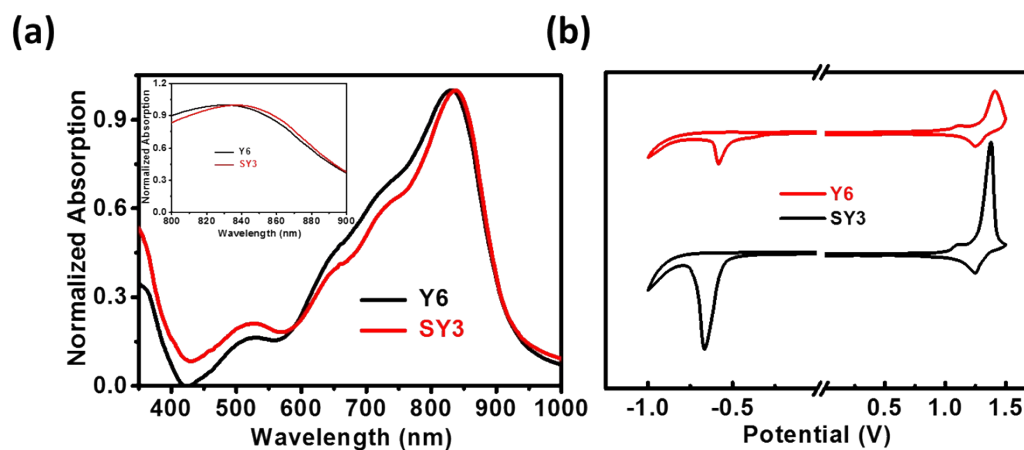


**Figure S9.** (a) Normalized UV-vis absorption spectra of neat Y6 and SY3 films; (b) The CV curves of Y6 and SY3.

**Table S5.** The photovoltaic parameters of the binary and ternary OSCs.

PM6:Y6:SY3	$V_{oc}$ (V)	$J_{sc}$ (mA cm <sup>-2</sup> )	FF	PCE <sup>a)</sup> (%) (ave.)
1:1.2:0	0.844	25.10 (24.75) <sup>b)</sup>	0.778	16.49 (16.11 ± 0.17)

1:1:0.2	0.855	25.51 (25.09)	0.782	17.07 (16.71 ± 0.23)
1:0:1.2	0.865	25.22 (24.91)	0.762	16.63 (16.23 ± 0.19)

a) PCEs in brackets are average values based on 20 independent devices; b) Values in brackets are calculated from IPCE.

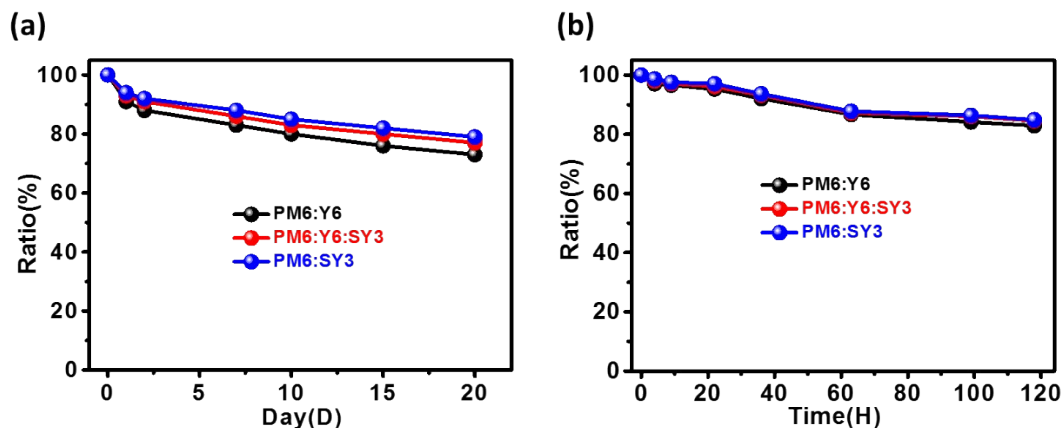


**Figure S10.** Device stability: (a) The PCE reduction of the packaged PM6:Y6, and PM6:SY3-based binary devices and the optimal ternary device during the 30 days in-air testing; (b) The photostability of packaged PM6:Y6, and PM6:SY3-based binary devices and the optimal ternary device during the 120 hours testing under LED flood light with a power of 150W.

#### Reference

1. T. Liu, Z. Luo, Fan, Q. Zhang, G. Zhang, L. Gao, W. Guo, X. Ma, W. Zhang, M. Yang, C. Yang, H. Yan, *Energy Environ. Sci.*, 2018, **11**, 3275.
2. H. Jiang, X. Li, Z. Liang, G. Huang, W. Chen, N. Zheng, R. Yang, *J. Mater. Chem. A*, 2019, **7**, 7760.
3. F. Pan, L. Zhang, H. Jiang, D. Yuan, Y. Nian, Y. Cao, J. Chen, *J. Mater. Chem. A*, 2019, **7**, 9798.
4. K. Li, Y. Wu, Y. Tang, M. Pan, W. Ma, H. Fu, C. Zhan, J. Yao, *Adv. Energy Mater.*, 2019, **9**, 1901728.
5. M. Zhang, W. Gao, F. Zhang, Y. Mi, W. Wang, Q. An, J. Wang, X. Ma, J. Miao, Z. Hu, X. Liu, J. Zhang, C. Yang, *Energy Environ. Sci.*, 2018, **11**, 841.

6. J. Song, C. Li, L. Zhu, J. Guo, J. Xu, X. Zhang, K. Weng, K. Zhang, J. Min, X. Hao, Y. Zhang, F. Liu and Y. Sun, *Adv. Mater.*, 2019, **31**, 1905645.
7. Y. Dong, Y. Zou, J. Yuan, H. Yang, Y. Wu, C. Cui and Y. Li, *Adv. Mater.*, 2019, **31**, 1904601.
8. T. Liu, Z. Luo, Y. Chen, T. Yang, Y. Xiao, G. Zhang, R. Ma, X. Lu, C. Zhan, M. Zhang, C. Yang, Y. Li, J. Yao, H. Yan, *Energy Environ. Sci.*, 2019, **12**, 2529.
9. C. Yan, T. Liu, Y. Chen, R. Ma, H. Tang, G. Li, T. Li, Y. Xiao, T. Yang, X. Lu, X. Zhan, H. Yan, G. Li, B. Tang, *Sol. RRL*, 2020, **4**, 1900377.
10. R. Ma, Y. Chen, T. Liu, Y. Xiao, Z. Luo, M. Zhang, S. Luo, X. Lu, G. Zhang, Y. Li, H. Yan, K. Chen, *J. Mater. Chem. C* **2020**, **8**, 909.
11. C. Wang, B. Jiang, J. Lu, M. -T. Cheng, R. Jeng, Y. -W. Lu, C. -P. Chen, K. -T. Wong, *ChemSusChem*, 2020, **13**, 903.